Load Governor for Fuel Cell Oxygen Starvation Protection: A Robust Nonlinear Reference Governor Approach

Jing Sun, *Fellow, IEEE,* and Ilya V. Kolmanovsky, *Senior Member, IEEE*

Abstract—The fuel cell oxygen starvation problem is addressed in this paper using a robust load governor. By regulating the current drawn from the fuel cell, the pointwise-in-time constraints on the oxygen excess ratio and on the oxygen mass inside the cathode are strictly enforced to protect the fuel cells from oxygen starvation. The load governor is designed using a nonlinear reference governor approach. Parameter uncertainties such as those due to imperfect controls of temperature and humidity are handled in the load governor design using a novel approach based on sensitivity functions. Simulation results are included to demonstrate the effectiveness of the proposed scheme. The results are compared with those of a linear filter which has been proposed in the prior literature to achieve similar goals.

Index Terms—Constrained optimization, fuel cells, load management, observer, reference governors.

I. INTRODUCTION

FUEL cell research has recently received a great deal of attention because of its strategic importance in global energy conservation and its positive impact on the environment. Successful and wide-spread commercial applications of fuel cell systems in transportation and power generation industries will alleviate the dependence of human society on fossil fuels and make the renewable resource a reality. However, challenging problems in the areas of material, manufacturing, fuel processing and distribution, and control need to be resolved before the cars propelled with fuel cells can be driven on the road.

Major control problems for fuel cell systems are highlighted in [1] and [2]. In this paper, we consider the load control of the fuel cells with the main focus on preventing oxygen starvation. Power generation in fuel cells relies on the continuous supply of oxygen to the cathode side and hydrogen to the anode side, when proper temperature and humidity conditions are maintained. The amount of power the fuel cells system delivers is controlled by the amount of current drawn from the system, if the proper conditions for cell operation are maintained. When a large load is applied to the cells, the sudden increase in the current can cause the system to stall if the depleted oxygen or hydrogen cannot be replenished immediately and sufficiently. The cell starvation can lead to system stall or permanent cell damage or reduced cell lifetime [2].

To protect the fuel cells from overloading and starvation, especially during the transient conditions, one can supply excessive oxygen and hydrogen to the cells during the steady-state operation, thus, increasing the reserve of available power in anticipation of the load increase. This strategy, however, is conservative, and it leads to increased parasitic losses, decreased air utilization and, thus, a compromised system performance. Another approach is to modify the load demand with a first-order or other slew-type filter [3], so that the application of the load is delayed to give time for the air and fuel supplies to catch up. While a filter can mitigate the problem and is easy to implement, it cannot guarantee that cell starvation is eliminated. When the filter is tuned for the worst-case scenario, it often leads to a conservative design with slow response. Other approaches, such as the model predictive control (MPC) [4], have also been proposed to address the issues.

In this paper, we formulate the fuel cells starvation protection as a constraint-enforcement problem. The reference governor [5], a mechanism effective in guaranteeing pointwise-in-time state and input constraints being satisfied, is explored for the load (current) governance. A load governor is designed to minimize the load tracking error while at the same time checking conditions for constraint violation. If constraint violation is predicted, the load will be reduced until all the constraints are satisfied. The computations involved in implementing the load governor include the simulations of the plant model over a finite time horizon and bisectional search for determining the optimal gain. Although the performance of the reference governor can be suboptimal as compared to more flexible MPC controllers, the computational implementation of the reference governor can be much simpler, which is a significant advantage for chronometrics and memory constrained automotive microcontrollers.

In dealing with the load control for the oxygen starvation protection problem, we first assume the temperature and humidity of the fuel cells are controlled around its setpoint with good accuracy. This allows us to use a nominal model for the load governor design and implementation. Given that the temperature and humidity controls represent some of the toughest challenges in fuel cell system management, this assumption most likely will be violated in real application. To mitigate the problems associated with model uncertainties, especially those caused by temperature and humidity fluctuation, we propose a robust load

J. Sun is with the Naval Architecture and Marine Engineering Department, University of Michigan, Ann Arbor, MI 48109 USA (e-mail: jingsun@umich.edu).

I. V. Kolmanovsky is with Powertrain Control Systems Department, Ford Research and Advanced Engineering, Dearborn, MI 48121 USA (e-mail: ikolmano@ford.com).

governor by taking into account explicitly the parametric uncertainties in our design. In particular, we incorporate three parameters in the model to represent uncertainties in: 1) the supply manifold relative humidity; 2) the vapor saturation pressure in the cathode due to temperature deviation, 3) the vapor diffusion across the membrane. In addition to the computations involved with the nominal load governor, i.e., the simulation of the nominal plant model and bisectional search, the robust load governor uses sensitivity functions for the linearized model and an estimate for the error bound for linearization to guarantee the robust performance.

The paper is organized as follows. A control oriented model based on [6] will be briefly presented in Section II, followed by a discussion on the control design objectives. Section III describes the load governor, which is based on the reference governor concept, for the fuel cell current control. A state observer, which provides the state estimation for the load governor, is also presented in Section IV. The robust load governor, aimed at guaranteeing constraint satisfaction under parametric uncertainties, is delineated in Section V. Section VI highlights the simulation results, where the performance of the robust load governor is compared with that of a regular reference governor and with the system that uses a first-order filter. Section VII concludes the paper with a brief summary.

For the sake of clarity, we limit the scope of this paper to preventing oxygen starvation by regulating the fuel cell current, with constraints imposed on the oxygen excess ratio and the amount of oxygen left in the cathode. For the fuel cell systems considered in this paper, the oxygen subsystem has slower dynamics compared with the hydrogen supply system, therefore oxygen starvation is the more obstinate problem during fast transient operation. However, the same scheme and design process can be extended to include additional constraints involving the conditions on the anode side with hydrogen starvation, or other conditions on the cathode side with compressor stall and surge. The robust load governor developed in this paper can also be extended to general cases which involve multiple uncertain parameters.

II. CONTROL DESIGN MODEL AND PROBLEM FORMULATION

A. Control-Oriented Model

This paper is primarily concerned with the oxygen starvation protection problem for proton exchange membrane fuel cells (PEMFC), although the concepts and techniques are not restricted to this system. A schematic drawing of the air supply system on the cathode side is shown in Fig. 1, where it includes the compressor, the temperature and humidity control loops and their actuators. The problem of PEMFC reactant control has been extensively studied, interested readers can refer to [7] and [8]. For the reactant flow control, the current drawn from the fuel cell is often considered as a disturbance, whose effects will be compensated by the air and fuel controllers. In this paper, however, we treat the electric load as controllable by the power conditioning unit, and a load governor is designed to manage the application of fuel cell load to protect the fuel cell system from starvation and to prolong its lifetime.
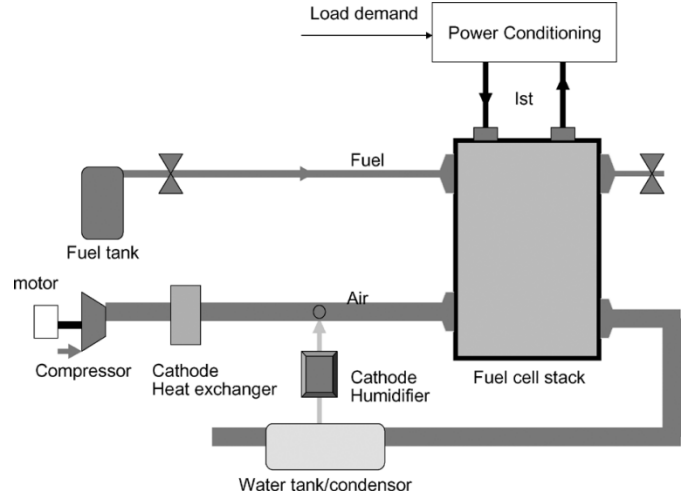

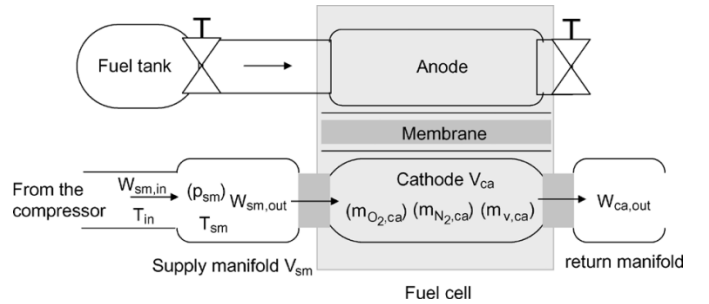Fig. 1. Fuel cell system schematics with key components.

Fig. 2. Illustrative fuel cell system diagram with key variables. The variables in parentheses are state variables.

Several control-oriented models have been developed and explored for PEMFC control design and system optimization. In this paper, the design of the load governor is based on the model developed in [6], where the dynamics of the supply and return manifolds, the characteristics for the cathode and anode, and the fuel cell auxiliaries are identified. To concentrate on the oxygen starvation protection, a four-state model for the air dynamics of the fuel cells model, simplified from the nine-state model of [6], is considered. The volumes modeled and the states used in the model are illustrated in Fig. 2, and the governing equations are given as

$$\dot{p}_{sm} = \frac{R_a}{M_{sm}V_{sm}}(W_{sm,\text{in}}T_{\text{in}} - W_{sm,\text{out}}T_{sm}) \quad (1)$$

$$\dot{m}_{O_2,ca} = W_{O_2,\text{in\_ca}} - W_{O_2,\text{out\_ca}} - W_{O_2,rct} \quad (2)$$

$$\dot{m}_{N_2,ca} = W_{N_2,\text{in\_ca}} - W_{N_2,\text{out\_ca}} \quad (3)$$

$$\dot{m}_{v,ca} = W_{v,\text{in\_ca}} - W_{v,\text{out\_ca}} + W_{v,\text{gen}} + W_{v,mbr} \quad (4)$$

where $R_a = 8313.3 J/(kmole \cdot K)$ is the universal gas constant for air, T, W, p, V denote the temperature, mass flow rate, pressure, and volume, respectively, and the subscript represents the variable taken at a specific location. For example, T_{sm} represents the supply manifold temperature, while $W_{sm,\text{in}}$, $W_{sm,\text{out}}$ denote the mass flow rate in and out of the supply manifold, M_{sm} is the mole weight of the gas in the supply manifold. $m_{O_2,ca}$, $m_{N_2,ca}$, $m_{v,ca}$ denote the total mass of oxygen, nitrogen, and vapor in the cathode. $W_{x,\text{in\_ca}}$, $W_{x,\text{out\_ca}}$ represent the mass flow rate of constituent x in and out of the cathode,

respectively. $W_{O_2,rct}$ represents the rate at which oxygen is consumed due to reaction, which is dictated by the stack current I_{st} through the relation

$$W_{O_2,rct} = M_{O_2}\frac{nI_{st}}{4F} \tag{5}$$

where n is the number of cells in the stack and $F = 96\,485$ is the Faraday number. $W_{v,gen}$, $W_{v,mbr}$ are the rates at which water (vapor) is generated due to H_2/O_2 reactions and transported across the membrane, respectively; their expressions can be found in [6].

Assuming the flows from the supply-to-cathode and cathode-to-return manifolds are controlled by linear nozzles, the flow rates W_x of different constituents in and out of the cathode are calculated using their partial pressures or mole fractions and orifice model. For example, with the relative humidity and temperature in the supply manifold controlled at ϕ_{sm} and T_{sm}, respectively, the total mass flow rate and the oxygen mass flow rate from the supply manifold to the cathode are given as

$$W_{ca\_in} = A_{sm2ca}(p_{sm} - p_{ca})$$
$$W_{O_2,ca\_in} = W_{ca\_in}\frac{p_{O_2,sm}M_{O_2}}{p_{sm}M_{sm}}$$

where M_{O_2}, M_{sm} are the mole weight of oxygen and gas mixture in the supply manifold, respectively, and $p_{x,sm}$ is the partial pressure of the constituent x in the supply manifold. The partial pressure of the oxygen in the supply manifold can be expressed as

$$p_{O_2,sm} = 0.21\,(p_{sm} - \phi_{sm}p_{sat}(T_{sm}))$$

where p_{sat} is the vapor saturation pressure which is a function of the temperature. Similar expressions can be obtained for all other terms in the model (1)–(4).

In addition to the plant model, we also assume that a Proportional+Integral (PI) feedback control, in combination with feedforward scheduling, is used to regulate the oxygen excess ratio, defined as

$$\lambda_o = \frac{W_{O_2,\text{in\_ca}}}{W_{O_2,rct}} \tag{6}$$

to a setpoint. We, thus, augment the plant model with the controller state to include the following dynamics

$$\dot{x}_c = e_\lambda$$
$$W_{sm,\text{in}} = K_{ff}(I_{st}) + K_p e_\lambda + K_i x_c \tag{7}$$

where $e_\lambda = \lambda_o - \lambda_o^s$ is the oxygen excess ratio regulation error, and K_{ff} is the feedforward term that will be scheduled based on the stack current I_{st}. The K_p, K_i are constant gains of the PI controller. The parameters K_{ff}, K_p, K_i are fixed from the outset for the load governor design. When these values change, only the underlying model used in the load governor implementation needs to be updated. All other algorithms and implementation for the load governor will remain the same, since they do not use the parameters in the model explicitly.

For the purpose of providing a self-contained description of the fuel cell model, all the equations implemented in the fuel cell model simulation, including those for the PI feedback controller, are summarized as follows:

$$\dot{p}_{sm} = \frac{R_a}{M_{sm}V_{sm}}(W_{sm,\text{in}}T_{\text{in}} - W_{sm,\text{out}}T_{sm})$$
$$\dot{m}_{O_2,ca} = W_{O_2,\text{in\_ca}} - W_{O_2,\text{out\_ca}} - W_{O_2,rct}$$
$$\dot{m}_{N_2,ca} = W_{N_2,\text{in\_ca}} - W_{N_2,\text{out\_ca}}$$
$$\dot{m}_{v,ca} = W_{v,\text{in\_ca}} - W_{v,\text{out\_ca}} + W_{v,\text{gen}} + W_{v,mbr}$$
$$\dot{x}_c = \frac{W_{O_2,\text{in\_ca}}}{W_{O_2,rct}} - \lambda_o^s$$
$$W_{sm,\text{in}} = K_{ff}(I_{st}) + K_p\left(\frac{W_{O_2,\text{in\_ca}}}{W_{O_2,rct}} - \lambda_o^s\right) + K_i x_c$$
$$W_{sm,\text{out}} = A_{sm2ca}(p_{sm} - p_{ca})$$
$$W_{O_2,\text{in\_ca}} = \frac{W_{sm,\text{out}}p_{O_2,sm}M_{O_2}}{p_{sm}M_{sm}}$$
$$W_{O_2,\text{out\_ca}} = \frac{W_{sm,\text{out}}m_{O_2,ca}}{m_{O_2,ca} + m_{N_2,ca} + m_{v,ca}}$$
$$W_{O_2,rct} = M_{O_2}\frac{nI_{st}}{4F}$$
$$W_{N_2,\text{in\_ca}} = \frac{W_{sm,\text{out}}p_{N_2,sm}M_{N_2}}{p_{sm}M_{sm}}$$
$$W_{N_2,\text{out\_ca}} = \frac{W_{ca,\text{out}}m_{N_2,ca}}{m_{O_2,ca} + m_{N_2,ca} + m_{v,ca}}$$
$$W_{v,\text{in\_ca}} = \frac{W_{sm,\text{out}}p_{v,sm}M_v}{p_{sm}M_{sm}}$$
$$W_{v,\text{out\_ca}} = \frac{W_{sm,\text{out}}m_{v,ca}}{m_{O_2,ca} + m_{N_2,ca} + m_{v,ca}}$$
$$W_{v,\text{gen}} = M_v\frac{nI_{st}}{2F}$$
$$W_{v,mbr} = 1.2684\frac{M_v A_{fc}nI_{st}}{F}$$
$$W_{ca,\text{out}} = A_{ca2rm}(p_{ca} - p_{rm})$$
$$p_{ca} = \frac{(m_{O_2,ca} + m_{N_2,ca} + m_{v,ca})R_a T_{ca}}{V_{ca}}$$
$$p_{O_2,sm} = 0.21(p_{sm} - p_{v,sm})$$
$$p_{N_2,sm} = 0.79(p_{sm} - p_{v,sm})$$
$$M_{sm} = \frac{p_{v,sm}M_v + p_{O_2,sm}M_{O_2} + p_{N_2,sm}M_{N_2}}{p_{sm}}.$$

The temperature in the supply manifold and cathode are assumed to be the same as the inlet, i.e., $T_{\text{in}} = T_{sm} = T_{ca} = 353$ K. The partial pressure of the vapor in the supply manifold is calculated as $p_{v,sm} = \phi_{sm}p_{v,sat}(T_{sm})$ where $p_{v,sat} = 47\,317$ Pa for $T_{sm} = 353$ K and a constant relative humidity ϕ_{sm} is used. The mole weights for different species are $M_{O_2} = 32$, $M_{N_2} = 28$, $M_v = 18$. Other physics and geometry related parameters used in (8) are from [6], i.e., $A_{fc} = 0.028$ m^2, $A_{sm2ca} = 0.0006$ m^2, $A_{ca2rm} = 0.0018$ m^2, $n = 381$, $F = 96\,485$, $V_{ca} = 0.01$ m^3, $V_{sm} = 0.02$ m^3, $\lambda_o^s = 2$, $n = 381$.

B. Design Objectives

At steady-state conditions, a fuel cell is operated at a fixed oxygen excess ratio λ_o^s ($\lambda_o^s = 2$ is used in this study) where an overall optimal system efficiency is achieved [9]. The regulation of λ_o is assumed to be achieved by the controller (7). During
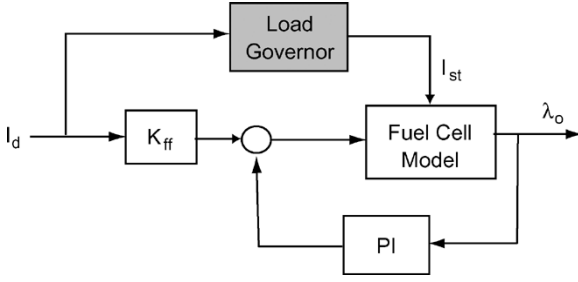
Fig. 3.   Fuel cell control systems with the load governor.

the transient when a large load[1] is suddenly applied, λ_o will temporarily drop below this setpoint, since the depleted oxygen cannot be immediately replenished due to manifold dynamics. Oxygen starvation is most likely to occur when λ_o falls too far below the setpoint for a sustained period of time. The risk of oxygen starvation is also increased when the oxygen mass in the cathode, $m_{O_2,ca}$, is too low.

Our objective is to design an add-on governor for the load application. Instead of applying the demanded current I_d immediately and directly to the fuel cell, we want to control the current which is drawn from the fuel cell so that:

- the applied load I_{st} tracks the demanded load I_d as closely as possible;
- the following constraints are satisfied for all time:

$$m_{O_2,ca} \geq m_{O_2,ca}^{\min}, \quad \lambda_o \geq \lambda_o^{\min}. \tag{8}$$

Since I_{st} will dictate how much oxygen will be depleted instantaneously, as shown in (5), the oxygen starvation can be effectively eliminated by preventing the load from drawing too much current from the cell stack.

## III. REFERENCE GOVERNOR FOR LOAD CONTROL

Reference governor is an add-on mechanism for enforcing constraints through a modified input [5]. It is a simple, yet effective scheme to avoid constraint violation for both linear and nonlinear systems. For the fuel cell oxygen starvation protection problem under consideration, the load governor serves as an interface between the commanded load and the applied load, as shown in Fig. 3. It accepts input commands and modifies their value so that: 1) all the constraints are satisfied; 2) the tracking error between the commands and actual inputs is minimized.

According to the reference governor concept [5], [10], the stack current I_{st} to be drawn from the fuel cells over the time interval $[kT, (k + 1)T]$, where T is the sample period, can be generated based on the current request, $I_d(kT)$, as follows:

$$\bar{I}_{st}(kT) = \bar{I}_{st}((k-1)T) + \beta(kT)$$
$$\times \left(I_d(kT) - \bar{I}_{st}((k-1)T) \right)$$
$$I_{st}(\tau) = \bar{I}_{st}(kT) \quad kT \leq \tau < (k+1)T. \tag{9}$$

The parameter $\beta(kT) \in [0,1]$ in (9) is maximized at each sample time k, subject to the condition that maintaining $I_{st}(\tau) = \bar{I}_{st}(kT)$ for $\tau \geq kT$ guarantees that the constraints will be satisfied for all $\tau \geq kT$.

[1]In this paper, the terms "load" and "current" are synonymous.
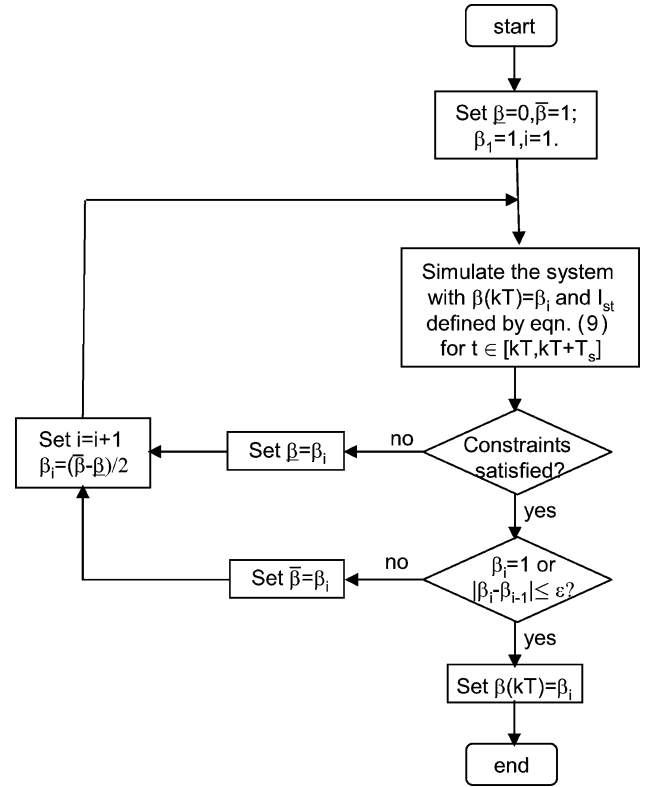
Fig. 4.   Bisectional search algorithm for determining $\beta(kT)$, where ϵ is the tolerance for convergence test.

To determine the parameter β at each time instant kT, the fuel cell model, including the controller dynamics (7), is simulated forward in time over the interval of $[kT, kT + T_s]$, where T_s is the simulation horizon. If the constraints are violated for any time during the simulated time period, $\beta(kT)$ will be reduced and simulation reinitiated. If all the constraints are satisfied for the simulated trajectory, the value of $\beta(kT)$ will be increased to minimize the tracking error between I_{st}, the current that is drawn from the fuel cell, and I_d, the current demanded by the load. The process will be repeated using the bisectional search[2] (see Fig. 4) until β converges.

Remark 1: For a general guideline, T_s should be selected so that if I_{st} is maintained at a constant value after the time instant t and the constraints are satisfied over the time interval $[t, t+T_s]$ then they will be also satisfied over the interval for any $T_a > T_s$. In general, it suffices to choose T_s to be 2–5 times the system time constant. Note that although larger T_s causes computational overhead to simulate the model, the dimensionality of the optimization problem to determine β does not change.

Remark 2: Simulating the model over the extended horizon $[kT, kT + T_s]$ is essential for the reference governor design. It assures that infeasible states are avoided and the constraint can be satisfied for all future time with some $\beta(kT) \in [0, 1]$. Note that the desired properties of a reference governor are established [5] with the assumption that maintaining $I_{st}(\tau) = \bar{I}_{st}(kT)$ for all $\tau \geq kT$ will guarantee that constraints can be satisfied for all $\tau \geq kT$. By choosing $I_{st}(kT)$ to satisfy all

[2]An alternative approach is to utilize a finite grid search, see [5] for conditions for the grid.

TABLE I
LINEARIZED MODEL FOR OBSERVER DESIGN

	$I_{st} = 150A$	$I_{st} = 250A$
A	$\begin{bmatrix} -1.3012 & 0.0000 & 0.0000 & 0.0000 \\ 3.8838 & -1.8001 & -0.8391 & -1.3704 \\ 12.7843 & -3.6257 & -5.3346 & -7.0469 \\ 0.4986 & -0.6879 & -0.8134 & -2.4515 \end{bmatrix}$	$\begin{bmatrix} -1.1209 & 0.0000 & 0.0000 & 0.0000 \\ 3.9249 & -2.2548 & -0.7958 & -1.3346 \\ 12.9195 & -3.3063 & -5.5222 & -6.7673 \\ 0.3223 & -0.5526 & -0.6691 & -2.7670 \end{bmatrix}$
C	$\begin{bmatrix} 1 & 0 & 0 & 0 \\ 0 & 0.0644 & -0.0030 & -0.0047 \end{bmatrix}$	$\begin{bmatrix} 1 & 0 & 0 & 0 \\ 0 & 0.0988 & -0.0025 & -0.0039 \end{bmatrix}$
$eig(A)$	$\{-7.3994, -1.3012, -1.1063, -1.0805\}$	$\{-7.3417, -1.6221, -1.5802, -1.1209\}$

the constraints in the time horizon $[kT, kT + T_s]$ and for all time $t \geq kT$ as implied by Remark 1, it guarantees that at least one feasible solution $(\beta = 0)$ exists for the next sampling time $(k + 1)T$.

Remark 3: The implementation of the load governor requires simulating the plant model multiple times at each sample time instant so that to optimize a single scalar parameter. Compared to other constraint-enforcing algorithms, such as the MPC, this computational demand is less stringent and can be more easily satisfied. The number of simulations can be controlled by changing the bisections stopping tolerance, while the time available to complete the simulations can be affected by the choice of T (which can be longer, if necessary, than the sampling period utilized for the PI controller updates). With a different implementation of the reference governor reliant on offline functional characterization of safe and strongly returnable sets [5], the online model simulations can be avoided. This approach can be particularly effective when the underlying model is linear [11], in which case the optimal solution for $\beta(kT)$ is computed by an explicit formula and the number of flops is known in advance.

IV. LOAD GOVERNOR WITH AN OBSERVER

The implementation of the load governor discussed in Section III requires that the states of the plant are accessible. At each sampling time kT, the state in the simulation model x is reset to the value of the plant state, and then the simulation is performed forward in time over the interval $[kT, kT + T_s]$.

Given that the gas constituent mass m_{O_2}, m_{N_2}, m_v inside the cathode cannot be measured, a state observer is constructed to provide the information necessary to implement the load governor. For the observer design, we assume that the supply manifold pressure p_{sm} and the fuel cell voltage v_{fc} are the measured outputs. As the following analysis shows, including v_{fc} as a measured variable is essential for the observability of the system.

In order to design and analyze the load governor using estimated states, we need to incorporate the polarization curve given by (10) into the fuel cell model. The expression is simplified from the general model developed in [6], where $\bar{p}_{cat}, \bar{p}_{O_2},$

$\bar{p}_{sat}$ are the total pressure, O_2 partial pressure, and vapor saturation pressure on the cathode side, in bars. i is the current density defined as $i = I_{st}/A_{fc}$, with A_{fc} being the fuel cell active area. These coefficients are derived for a specific 5 kW fuel cell system [6], but the structure of the model is more generic

$$v_{fc} = 1.16 - 0.2804i - \left(-0.2121 - 0.1706\frac{\bar{p}_{O_2}}{0.1173} \right.$$
$$\left. + 0.0392\left(\frac{\bar{p}_{O_2}}{0.1173}\right)^2 \right) i^3$$
$$- \left(\left(0.2162 + 0.0228 log\left\{ \frac{\bar{p}_{ca} - \bar{p}_{sat}}{1.013} \right\} \right) \right.$$
$$+ \left(0.0105\left(\frac{\bar{p}_{O_2}}{0.1173} + \bar{p}_{sat}\right)^2 \right.$$
$$\left. -0.1025\left(\frac{\bar{p}_{O_2}}{0.1173} + \bar{p}_{sat}\right) + 0.3689 \right)$$
$$\times (1 - e^{-10i})). \tag{10}$$

The linearized models of the fuel cell system with $x = [p_{sm}, m_{O_2,ca}, m_{N_2,ca}, m_{v,ca}]^\top$, $y = [p_{sm}, v_{fc}]^\top$ at two different operating points are shown in Table I. It can be shown that the system is not observable with p_{sm} as the only output. On the other hand, by including v_{fc} as one of the outputs, the system is observable for all operating conditions. Given that the open-loop system is stable (as shown in Table I for two representative operating points), open-loop state observer can be incorporated to provide the state information needed for implementing the load governor. In this study, a closed-loop Luenberger observer with fixed gain is used to improve the performance of the state estimation. The observer is designed using the linear model at $I_{st} = 250$ and then validated for other operating conditions. As shown in Fig. 5, the closed-loop Luenberger observer can reduce the observer error and provide the required information for the reference governor implementation.

More detailed analysis of fuel cell observer design can be found in [9] and [12].

V. ROBUST LOAD GOVERNOR

The difficulties in precisely controlling the temperature and humidity of the fuel cell air delivery system are well appreciated by the fuel cell control community. When temperature and
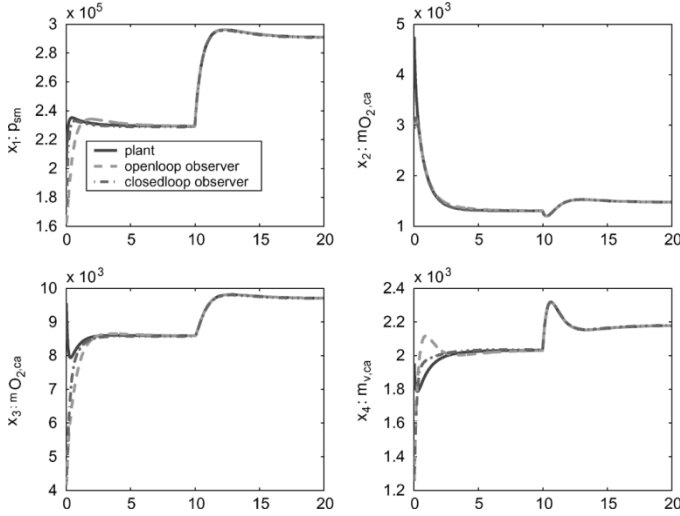
Fig. 5.   State estimates with open- and closed-loop observers.

humidity deviate from their set-points, the objective of the constraint enforcement may not be achieved with the regular load governor developed in Section III. On the other hand, the use of observer for state estimation will inevitably introduce additional error in the load governor implementation. The uncertainties we face in the fuel cell model and the need to incorporate state estimation error motivate us to seek improvement of the nominal load governor design to guarantee the robustness with respect to constraint satisfaction. We refer to the resulting scheme as a robust load governor.

If $\theta \in \Theta$ is a vector of uncertain parameters and Θ is a compact set, then in selecting $\beta(kT)$ in (9), the conditions that constraints are satisfied for $\tau \geq kT$ with $I_{st}(\tau) = \bar{I}_{st}(kT)$ must be guaranteed for all $\theta \in \Theta$. There are intricacies in the reference governor design for systems with parametric uncertainties. They have to be considered to rigorously guarantee constraint enforcement and assure the desired response properties of the reference governor [5]. First, no feasible $\beta(kT) \in [0,1]$ may exist at some time instants kT even if a feasible initial $\beta(0)$ does exist. In this situation, $\beta(kT)$ must be set to zero. Second, to theoretically guarantee the desirable response properties of the reference governor such as finite-time convergence of $\bar{I}_{st}$ to I_d (so that the reference governor becomes inactive in finite time) the algorithm to compute $\beta(kT)$ has to be slightly modified [5]. Third, computational procedures are needed to check the constraints *for all* $\theta \in \Theta$.

To address the last issue, we now describe an approximate procedure which can efficiently handle the constraint checking for general nonlinear systems. We will afterwards discuss its applications to the fuel cell oxygen starvation protection problem. It should be pointed out that when the constraints are satisfied for all $\theta \in \Theta$ and $\tau \in [t, t + T_s]$, we can guarantee that $\beta(kT) \in [0,1]$ will always exist for $kT \geq t$, and therefore the first issue mentioned previously can be addressed as well.

Let us consider a general nonlinear system represented by

$$\dot{x} = f(x, r, \theta)$$
$$z = g(x, r, \theta) \qquad (11)$$

where x, r, θ are vectors of the states, reference inputs, and uncertain parameters, respectively, while z is the vector of variables subject to pointwise-in-time constraints. To implement the robust load governor, we need a computational procedure to determine, for given $x(0)$ and r, whether the constraints, written as $z(t) \in \mathcal{C}_z$ for $0 \leq t \leq T_s$, are satisfied for all $\theta \in \Theta$. During the reference governor operation, this procedure is to be applied at each time instant kT with the current state of the system in place of $x(0)$ and with r set to the proposed reference governor output.

Suppose $\theta_0 \in \Theta$ and let $x_n(t)$, $z_n(t)$, be the simulated trajectory of states and constrained variables, respectively, i.e.

$$\dot{x}_n = f(x_n, r, \theta_0)$$
$$z_n(t) = g(x_n(t), r, \theta_0).$$

For $\theta \in \Theta$, $\theta \neq \theta_0$, $z(t)$ can be approximated by $z_f(t)$ which is defined by

$$z_f(t) = z_n(t) + (\delta_\theta^z(t))^T (\theta - \theta_0) \qquad (12)$$

where δ_θ^z is the sensitivity function of z with respect to the parameter θ around the nominal trajectory x_n, z_n, i.e., $\delta_\theta^z = (\partial z / \partial \theta)|_{\theta=\theta_0}$. Assuming that f and g are sufficiently smooth, the sensitivity function can be computed as a solution to the following linearized matrix differential equation [14]:

$$\dot{x}_\theta = \frac{\partial f}{\partial x}\bigg|_{(x=x_n, \theta=\theta_0)} x_\theta + \frac{\partial f}{\partial \theta}\bigg|_{(x=x_n, \theta=\theta_0)}$$
$$\delta_\theta^z = \frac{\partial g}{\partial x}\bigg|_{(x=x_n, \theta=\theta_0)} x_\theta + \frac{\partial g}{\partial \theta}\bigg|_{(x=x_n, \theta=\theta_0)}$$
$$x_\theta(0) = 0. \qquad (13)$$

From (12) and based on Taylor's theorem [13], the condition $z(t) \in \mathcal{C}_z$ for all $\theta \in \Theta$ can be replaced by the following condition:

$$z_n(t) + (\delta_\theta^z(t))^T (\theta - \theta_0) + M\|\theta - \theta_0\|^2 \mathcal{B} \subset \mathcal{C}_z \forall \theta \in \Theta \quad (14)$$

where $\mathcal{B}$ is the unit ball. If $M > 0$ is sufficiently large and (14) holds for $0 \leq t \leq T_s$ then it implies $z(t) \in \mathcal{C}_z$ for $0 \leq t \leq T_s$. Since the left-hand side of the inclusion (14) is quadratic in θ, (14) can be easily verified with computations provided $\mathcal{C}_z$ and Θ have simple representations (such as parallelotopes or ellipsoids). To even further simplify the computations the term $M\|\theta - \theta_0\|^2 \mathcal{B}$ may be replaced by $M \max_{\theta \in \Theta} \|\theta - \theta_0\|^2 \mathcal{B}$, but this may lead to a more conservative reference governor performance.

For the fuel cell starvation protection problem addressed in this paper, since the constraints are imposed as lower bounds for λ_o and $m_{O_2,ca}$ and the uncertainties are assumed to be bidirectional (i.e., they can be larger or smaller than the nominal value) within a bound, condition (14) can be checked by a simple algorithm as

$$z_{ni}(t) - \sum_{j=1}^{3} \left|\delta_{\theta_j}^z(t)\right| max\{|\theta_j - \theta_{0j}|\} - \epsilon \geq z_i^{\min}, \quad i = 1, 2$$
$$(15)$$

where $z_{n1} = \lambda_o$, $z_{n2} = m_{O_2,ca}$ (with nominal parameters) and $\epsilon = M \max_{\theta \in \Theta} \|\theta - \theta_0\|^2 \mathcal{B}$ is a small high-order residual term.

The robust reference governor based on (14) is applied to the oxygen starvation protection problem with $\theta = [\theta_1, \theta_2, \theta_3]^T$, where $\theta_1 = \phi_{sm}$, $\theta_2 = p_{sat}$, and θ_3 is the multiplier to the membrane vapor diffusion term ($W_{v,mbr}$ in (4)). The relative humidity in the supply manifold, ϕ_{sm} is assumed to have uncertainty up to 50%; the vapor saturation pressure, which is highly dependent on the temperature, can vary up to 25 kPa (this corresponds to about 10 °C change in the temperature if the stack is operating around 80 °C); the membrane vapor diffusion coefficient is assumed to vary up to 50%.

The implementation of the robust load governor requires simulating the original plant model with the nominal parameters (for $z_{n1} = \lambda_o(t)$ and $z_{n2} = m_{O_2}(t)$) and the four sensitivity functions of $\partial \lambda_o / \partial \phi_{sm}$, $\partial \lambda_o / \partial p_{sat}$, $\partial m_{O_2,ca} / \partial \phi_{sm}$, $\partial m_{O_2,ca} / \partial p_{sat}$ over the time horizon of $T_s = 5$ s. The sensitivity functions are generated around the nominal trajectory $\lambda_o(t)$ and $m_{O_2}(t)$ using the linearized model (13). The linearized model for the fuel cells system was obtained using automated symbolic differentiation programmed with MATLAB.[3] The error between the nonlinear and the linearized system is taken into account through the incorporation of the M-term in (14).

Remark 4: The constant M in (14) can be estimated analytically or numerically. Analytical estimation of M requires the evaluation of the second-order sensitivity functions, and it could be very tedious when multiple uncertain parameters are involved. In our implementation, M was treated as a calibratable parameter, and was tuned until the constraints were satisfied for the worst case.

Remark 5: If the set Θ has a large diameter, it may be partitioned as $\Theta = \bigcup_{i=1,\dots,N} \Theta^i$, $N \geq 1$. Given $\theta_0^i \in \Theta^i$, $i = 1, \cdots, N$, the condition (14) can be replaced by the following N conditions:

$$z_n^i(t) + \left(\delta_\theta^{z,i}(t)\right)^T \left(\theta - \theta_0^i\right) + M^i \left\|\theta - \theta_0^i\right\|^2 \mathcal{B} \subset \mathcal{C}_z$$
$$\forall \theta \in \Theta^i. \tag{16}$$

Here $z_n^i(t)$ is the ith nominal trajectory of the constrained variables corresponding to $\theta = \theta_0^i$, $(\delta_\theta^{z,i}(t))$ is the sensitivity along the state trajectory corresponding to $\theta = \theta_0^i$, and $M^i > 0$ is a constant. If the sets Θ^i have small diameters then small M^i suffice so that the conservatism of the reference governor based on (14) can be mitigated. On the other hand, multiple online simulations of the nominal model and of the linearized system are needed, which increases the computational overhead.

Remark 6: If the state of the fuel cells system can only be estimated with a known error bound (e.g., it is only known that $x(0) \in X$), (14) can be modified to

$$z_n(t) + (\delta_\theta^z(t))^T (\theta - \theta_0) + \left(\delta_{x_0}^z(t)\right)^T (x(0) - x_0)$$
$$+ \left(M_1 \|\theta - \theta_0\|^2 + M_2 \|x - x_0\|^2\right) \mathcal{B} \subset \mathcal{C}_z, \quad \forall \theta \in \Theta \tag{17}$$

where $(\delta_{x_0}^z(t))^T$ is the initial condition sensitivity function computed using matrix differential equations similar to (13), while $M_1 > 0$ and $M_2 > 0$ are sufficiently large and $x_0 \in X$.

Remark 7: Other uncertainties, such as that in the flow coefficient, also exist in the fuel cell model and need to be properly

---

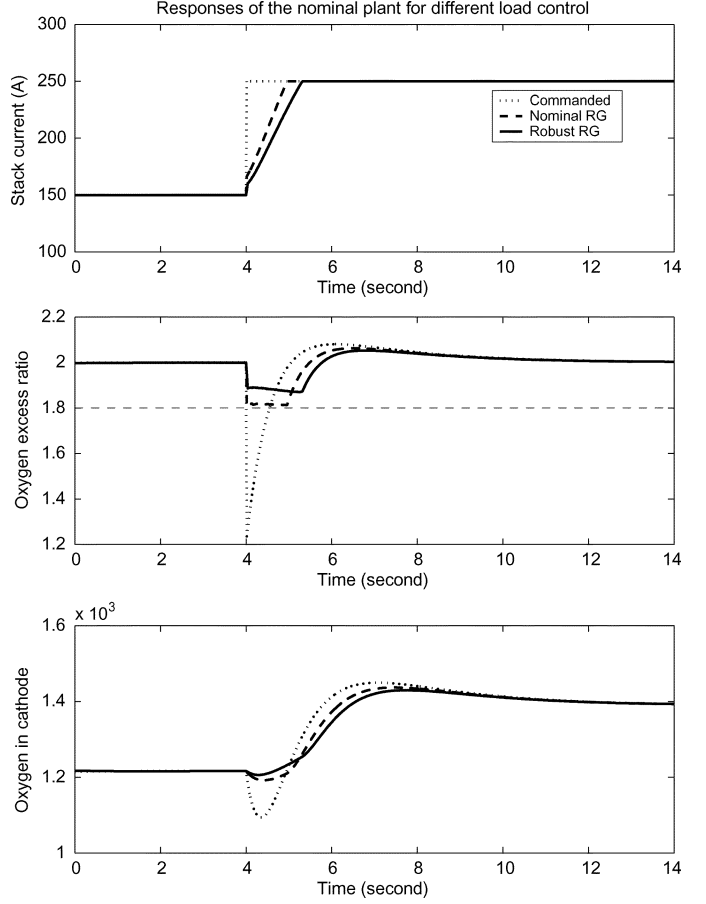[3]MATLAB is a registered trademark of the Mathworks, Inc., Natick, MA.

Fig. 6. Comparison of different load governors and their performance when applied to the nominal model.

addressed. The robust load governor described in this section can be expanded to include other parameter uncertainties by calculating additional sensitivity functions. In many applications, however, the uncertainties in flow coefficient can be compensated through feedback using measured flow rates.

VI. SIMULATION RESULTS AND COMPARISON

Both the nominal load governor (described in Section III) and the robust load governor (developed in Section V) are now applied to the fuel cells model. The simulated steps represent a 67% change in the load demand. Simulation results are summarized and analyzed in this section, and compared to the conventional load filtering approaches.

Fig. 6 shows the responses of the oxygen excess ratio and cathode oxygen mass for the system with the nominal parameter values, to (a) the commanded current; (b) the modified current with a nominal load governor; and (c) the modified current with a robust load governor. The constraints for the oxygen excess ratio and cathode oxygen mass are satisfied by both load governors (b) and (c), while the same constraints are violated for the direct application of the current command without a load governor.

Fig. 7 shows the results when the same load change is applied to the system with perturbed parameters. In this case, both constraints are violated if no load governor is used. The nominal ref-

Fig. 7. Comparison of different load governors and their performance when applied to a perturbed model.

Fig. 8. Load governors with infeasible intermediate steps when applied to a perturbed model.

erence governor (b), which is designed for θ_0 without checking constraint violation conditions for other values of $\theta \in \Theta$, cannot enforce the constraint on the oxygen excess ratio. The robust load governor (c), on the other hand, gives a smooth trajectory while satisfying all the constraints. The tracking performance for both the regular and the robust load governors, when applied to the perturbed system, is similar and therefore the tracking performance is not compromised in this case for achieving system robustness.

If the constraint on the oxygen excess ratio is relaxed (say from 1.8 to 1.6) and the closed-loop PI control system is not designed to be fast enough, we can observe another set of characteristics of the reference governor control. In this case, the nominal reference governor, which does not consider uncertainties in the plant model, might apply the load too aggressively during the transient that leads to the subsequent intermediate steps where no feasible solution for β can be found and therefore β is set to 0. This results in the jittering trajectory as shown in Fig. 8 when β has to be set to zero at these points. Meanwhile, the constraints are slightly violated. The intermediate infeasible steps are avoided with the robust load governor, as shown in Fig. 8 whose trajectory is smooth and constraints are satisfied.

Comparing Fig. 8 and Fig. 7 we also see that the current response by the reference governor is slower for the slower feedback control system; this underscores the dependence of the reference governor response properties on the feedback control system design. With a fast closed-loop system the constraints
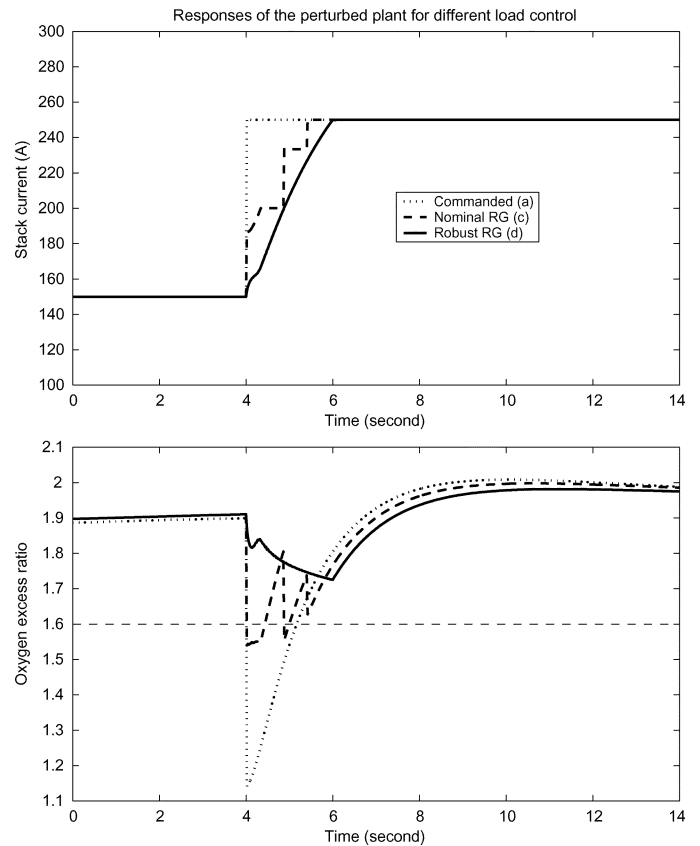
are typically active only for the initial few time instants in the predicted response, and the behavior of the reference governor is typically more regular, similar to that of a nonlinear rate limiter. This observation seems to hold for problems similar to the one at hand but it may not hold for other types of systems and constraints, e.g., for systems with stringent control constraints.

One could argue that a first-order linear filter on the current command instead of a reference governor may be sufficient if its time constant is tuned appropriately to satisfy the constraints. Fig. 9 shows the results when the time constant is adjusted to meet the constraints for the nominal plant ($\tau_f = 0.7$ s) and for the perturbed plant ($\tau_f = 1.2$ s). The load response in both cases is compared to the reference governor approach. The results are also summarized in Table II. Since the first-order filter involves no feedback, the robustness of constraint enforcement property has to be satisfied by a conservative filter with slow time constant, which will necessarily lead to compromised tracking performance, as shown in Table II.

Remark 8: The reference governor can be also viewed as a nonlinear filter, whose time constant is adjusted as a function of system states. As such, the reference governor adjusts the input to the fuel cells system only when it is necessary, i.e., when constraint violation is predicted over the horizon. As a consequence of the state-feedback, the performance of the load governor will change as the underlying plant changes, as shown in Table II. This is in contrast to the linear filter case when the same filtering mechanism is applied indiscriminately to all incoming commands. In particular, the response to even small load
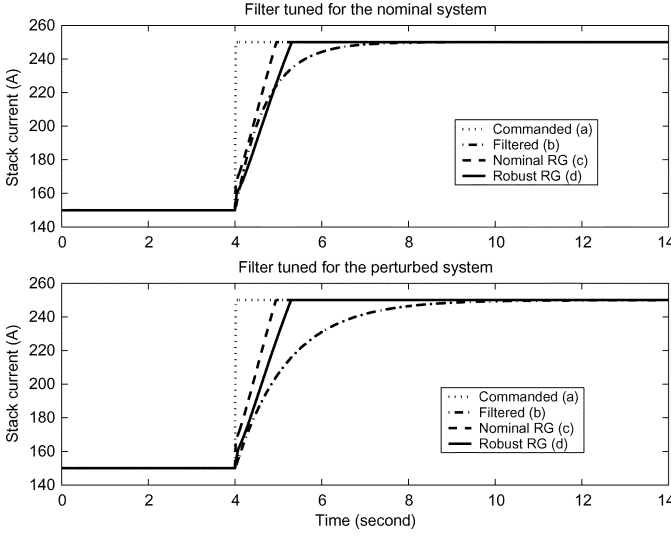
Fig. 9. Comparison of different load governors and their performance when applied to a perturbed model, when the filter time constant is calibrated to satisfy constraints for the nominal plant and the perturbed plant, respectively.

TABLE II
PERFORMANCE OF DIFFERENT LOAD GOVERNORS

		Constraints satisfied?		Tracking	
		P_0	P_Δ	P_0	P_Δ
No governor		NO	NO	0	0
With filter	$\tau_f = 0.4$	NO	NO	1	1
	$\tau_f = 0.7$	Yes	NO	1.75	1.75
	$\tau_f = 1.2$	Yes	Yes	3.002	3.002
Nominal LG		Yes	NO	1.185	1.17
Robust LG		Yes	Yes	1.919	1.923

Note: (1) P_0 and P_Δ represents the nominal and perturbed plants, respectively. (2) The tracking performance is measured by the integral of squares of the load tracking error, i.e., $\int_0^T (I_{st} - I_d)^2 dt$. For comparison, the numbers shown in this table are normalized by the performance achieved by a first-order filter with $\tau_f = 0.4$.

changes when no danger of constraint violation exists will be compromised. When the same constraint enforcing performance is achieved, the reference governor out-performs the first-order filter in terms of load tracking, due to its built-in optimization function. This benefit is achieved at the cost of a moderate computational effort.

Remark 9: When onboard computational resources are limited and the application of real-time optimization is prohibitive, the load governor developed in this paper can also be used off-line as a calibration tool to help optimize other load control strategies, such as gain scheduled filters or rate limiters. From Fig. 9, one can see that the response of the filter that satisfies the constraints should not rise faster than the reference governor for this application. This can be used as a guideline in selecting the filter time constant. It may also be possible to precompute the reference governor parameter, β, offline for different states and references and then approximate it with a nonlinear function (such as a neural network); this nonlinear function can subsequently be used for online implementation of the reference governor.

Remark 10: The load governor, like any other governance mechanism, will slow down the system response in order to deal with tight and active constraints. If the tracking performance is as imperative as the constraint enforcement requirement, then a compromise has to be made, or an additional power source, such as a battery or a super capacitor, has to be incorporated to meet both the load demand and the constraints. In this case, the reference governor can provide the information on the power deficit of the fuel cells systems, thus, offer the guidelines for the sizing of the auxiliary power unit.

Remark 11: When the parametric uncertainties are deterministic, the conservativeness of the robust load governor can be reduced by combining the robust load governor with an online parameter identification.

VII. CONCLUSION

In this paper, we applied the reference governor to the fuel cell oxygen starvation protection problems. The main advantage of the proposed scheme is that it enforces constraints with a minimum impact on system response time. The robust load governor, which takes into account the parametric uncertainties in the plant model, has shown robust performance with considerable parameter variation. The algorithm requires more computational resource for online implementation than a simple filter. On the other hand, it provides guaranteed constraint enforcement and improved load tracking performance.

REFERENCES

[1] S. Varigonda, J. T. Pukrushpan, and A. G. Stefanopoulou, "Challenges in fuel cell power plant control: the role of system level dynamic models," in *Proc. AIChE Spring Meeting*, 2003.
[2] W. C. Yang, B. Bates, N. Fletcher, and R. Pow, "Control Challenges and Methodologies in Fuel Cell Vehicle Development," , 1998, SAE Paper 98C054.
[3] Y. Guezennec and T. Y. Choi, "Supervisory control of fuel cell vehicles and its link to overall system efficiency and low-level control requirements," in *Proc. Amer. Control Conf.*, Denver, CO, 2003, pp. 2055–2061.
[4] A. Vahidi, A. G. Stefanopoulou, and H. Peng, "Model predictive control for starvation prevention in a hybrid fuel cell system," in *Proc. Amer. Control Conf.*, Boston, MA, Jun. 2004, pp. 834–839.
[5] E. G. Gilbert and I. V. Kolmanovsky, "Nonlinear tracking control in the presence of state and control constraints: a generalized reference governor," *Automatica*, vol. 38, no. 12, pp. 2063–2073, 2002.
[6] J. T. Pukrushpan, A. G. Stefanopoulou, and H. Peng, "Modeling and control for PEM fuel cell stack system," in *Proc. Amer. Control Conf.*, Anchorage, AK, 2002, pp. 3117–3122.
[7] J. Larminie and A. Dicks, *Fuel Cell Systems Explained*. New York: Wiley, 2000.
[8] J. T. Pukrushpan, A. G. Stefanopoulou, and H. Peng, "Control of fuel cell breathing," *Control Syst. Mag.*, pp. 30–46, Apr. 2004.
[9] ——, *Control of Fuel Cell Power Systems: Principles, Modeling, Analysis and Feedback Design*, Germany: Springer, 2004.
[10] A. Bemporad, "Reference governor for constrained nonlinear systems," *IEEE Trans. Autom. Control*, vol. 43, no. 3, pp. 415–419, Mar. 1998.
[11] E. G. Gilbert and I. V. Kolmanovsky, "Fast reference governors for systems with state and control constraints and disturbance inputs," *Int. J. Robust Nonlinear Control*, vol. 9, no. 15, pp. 1117–1141, 1999.
[12] M. Arcak, H. Gorgun, L. Pedersen, and S. Varigonda, "A nonlinear observer design for fuel cell hydrogen estimation," *IEEE Trans. Contr. Syst. Technol.*, vol. 12, no. 1, pp. 101–110, May 2004.
[13] E. G. Gilbert, "Functional expansions for the response of nonlinear differential systems," *IEEE Trans. Autom. Control*, vol. AC-22, no. 6, pp. 909–921, Dec. 1977.
[14] P. A. Ioannou and J. Sun, *Robust Adaptive Control*. Englewood Cliffs, NJ: Prentice-Hall, 1996.

Jing Sun (S'87–M'89–SM'00–F'04) received the Ph.D. degree from University of Southern California, Los Angeles, in 1989, and the B.S. and M.S. degrees from the University of Science and Technology, Hefei, China, in 1982 and 1984, respectively.

From 1989 to 1993, she was an Assistant Professor in the Electrical and Computer Engineering Department, Wayne State University, Detroit, MI. She joined Ford Research Laboratory in 1993, where she worked in the Powertrain Control Systems Department. After spending almost 10 years in industry, she came back to academia and joined the faculty of the College of Engineering, University of Michigan, Ann Arbor, in 2003, as an Associate Professor. Her research interests include system and control theory and its applications to marine and automotive propulsion systems. She holds over 30 US patents and has coauthored a textbook on Robust Adaptive Control.

Dr. Sun is one of the three recipients of the 2003 IEEE Control System Technology Award.

Ilya V. Kolmanovsky (S'94–M'95–SM'04) studied as an undergraduate at Moscow Aviation Institute, Russia. He received the M.S. degree and the Ph.D. degree in aerospace engineering, in 1993 and 1995, respectively, and the M.A. degree in mathematics, in 1995, all from the University of Michigan, Ann Arbor.

He is currently a Technical Leader in Powertrain Control at Ford Research & Advanced Engineering of Ford Motor Company, Dearborn, MI. In addition to expertise in the automotive engine and powertrain control, his research interests include potential of advanced control techniques as an enabling technology for advanced automotive systems, and several areas of control theory, which include constrained control, optimization-based and model-predictive control, and control of nonlinear mechanical, nonholonomic, and underactuated systems.

Dr. Kolmanovsky is the Chair of IEEE CSS Technical Committee on Automotive Control. He has served as an Associate Editor of IEEE CSS Conference Editorial Board (1997–1999), IEEE TRANSACTIONS ON CONTROL SYSTEMS TECHNOLOGY (2002–2004), IEEE TRANSACTIONS ON AUTOMATIC CONTROL (2005–present), and he was a Program Committee Member of American Control Conference in 1997, 1999, and 2004. He is the recipient of 2002 Donald P. Eckamn Award of American Automatic Control Council for contributions to nonlinear control and for pioneering work in automotive engine control of powertrain systems and of 2002 IEEE TRANSACTIONS ON CONTROL SYSTEMS TECHNOLOGY Outstanding Paper Award.